European Journal of Cardio-Thoracic Surgery 2023, 63(5), ezad115
https://doi.org/10.1093/ejcts/ezad115 Advance Access publication 23 March 2023

ORIGINAL ARTICLE

Cite this article as: Iwasieczko A, Gaddam M, Gaweda B, Goodyke A, Mathur M, Lin C-Y *et al*. Valvular complex and tissue remodelling in ovine functional tricuspid regurgitation. Eur J Cardiothorac Surg 2023; doi:10.1093/ejcts/ezad115.

Valvular complex and tissue remodelling in ovine functional tricuspid regurgitation

Artur Iwasieczko [a,b], Manikantam Gaddam[c], Boguslaw Gaweda[a,b], Austin Goodyke[c], Mrudang Mathur[d], Chien-Yu Lin[d], Joseph Zagorski[c], Monica Solarewicz[a], Stephen Cohle[e], Manuel Rausch[d] and Tomasz A. Timek [a,*]

[a] Division of Cardiothoracic Surgery, Spectrum Health, Grand Rapids, MI, USA
[b] Department of Cardiac Surgery, State Clinical Hospital Number 2, University of Rzeszow, Rzeszow, Poland
[c] Research Department, Spectrum Health, Grand Rapids, MI, USA
[d] Department of Biomedical Engineering, University of Texas at Austin, Austin, TX, USA
[e] Department of Pathology, Spectrum Health, Grand Rapids, MI, USA

* Corresponding author. Division of Cardiothoracic Surgery, Spectrum Health, 100 Michigan Ave SE, Grand Rapids, MI 49503, USA.
E-mail: tomasz.timek@spectrumhealth.org (T.A. Timek).

Received 19 September 2022; received in revised form 6 March 2023; accepted 22 March 2023

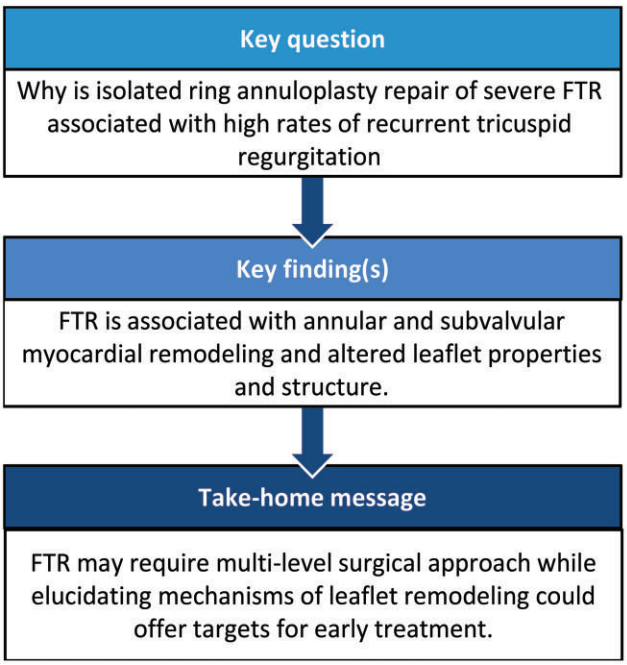

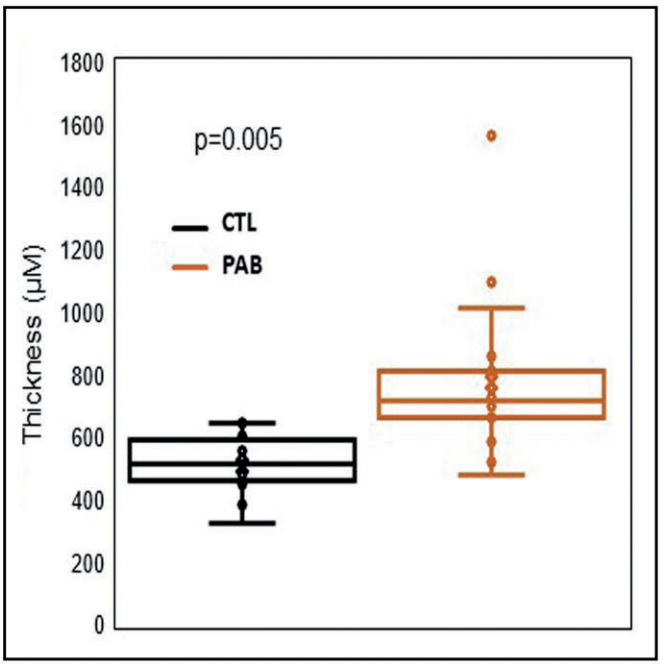

Abstract

OBJECTIVES: Pathophysiology of function tricuspid regurgitation (FTR) is incompletely understood. We set out to comprehensively evaluate geometric and tissue remodelling of the tricuspid valve complex in ovine FTR.

METHODS: Twenty adult sheep underwent left thoracotomy and pulmonary artery banding (PAB) to induce right heart pressure overload and FTR. After 8 weeks, 17 surviving animals and 10 healthy controls (CTL) underwent sternotomy, echocardiography and implantation of sonomicrometry crystals on right ventricle and tricuspid valvular apparatus. Haemodynamic and sonomicrometry data were acquired in all animals after weaning from cardiopulmonary bypass. Leaflet tissue was harvested for pentachrome histologic analysis and biomechanical testing.

RESULTS: Animal weight was 62 ± 5 and 63 ± 3 kg for CTL and PAB, respectively (P = 0.6). At terminal procedure, systolic pulmonary artery pressure was 22 ± 3 and 40 ± 7 mmHg for CTL and PAB, respectively (P = 0.0001). The mean TR grade (+0–4) was 0.8 ± 0.4 and 3.2 ± 1.2 (P = 0.0001) for control and banded animals, respectively. Right ventricle volume (126 ± 13 vs 172 ± 34 ml, P = 0.0019), tricuspid annular area (651 ± 109 vs 865 ± 247 mm^2, P = 0.037) and area between papillary muscle tips (162 ± 51 vs 302 ± 75 mm^2, P = 0.001) increased substantially while systolic excursion of anterior leaflet decreased significantly (23.8 ± 6.1° vs 7.4 ± 4.5°, P = 0.001) with banding. Total leaflet surface area increased from 806 ± 94 to 953 ± 148 mm^2 (P = 0.009), and leaflets became thicker and stiffer.

CONCLUSIONS: Detailed analysis of the tricuspid valve complex revealed significant ventricular, annular, subvalvular and leaflet remodelling to be associated with ovine functional tricuspid regurgitation. Durable surgical repair of severe FTR may require a multi-level approach to the valvular apparatus.

Keywords: Tricuspid valve • Functional tricuspid regurgitation • Valve repair

ABBREVIATIONS

CPB	Cardiopulmonary bypass
CTL	Control
ED	End diastole
ES	End systole
FTR	Functional tricuspid regurgitation
PAB	Pulmonary artery banding
RA	Right atrium
RV	Right ventricle

INTRODUCTION

The tricuspid valve is often referred to as the 'forgotten valve', but a recent large-scale population study deemed tricuspid regurgitation a 'public health crisis' [1] emphasizing the severe under appreciation of its incidence and infrequent surgical treatment. Current surgical therapy of functional TR is centred on reductive ring annuloplasty of the tricuspid annulus [2], but this strategy has been shown to be inadequate in the presence of severe TR with high rates of residual [3] and recurrent [4] insufficiency. The failure of annular reduction to successfully treat severe functional tricuspid regurgitation (FTR) emphasizes our incomplete understanding of the pathophysiology of right ventricular, annular, subvalvular and leaflet alterations in the evolution of TR. A more comprehensive and integrated evaluation of the TV complex in the setting of FTR is needed to improve our understanding of this vexing disease and potentially inform novel strategies for medical and surgical therapy. With this goal in mind, we set out to investigate tricuspid valvular complex remodelling associated with right ventricular failure and FTR induced by pulmonary artery banding (PAB) in adult sheep.

MATERIALS AND METHODS

Ethics statement

The study protocol was approved by Michigan State University Institutional Animal Care and Use Committee protocol number 2020-35 approved on 27 July 2020. All animals received humane care in compliance with the Principles of Laboratory Animal Care formulated by the National Society for Medical Research.

Surgical preparation

PAB animals (n = 20) underwent both the PAB procedure and the terminal procedure for the implantation of sonomicrometry crystals, while control animals (CTL, n = 10) underwent the terminal procedure only.

Pulmonary artery banding

Twenty Dorset healthy adult male sheep (63 ± 3kg) had external right jugular intravenous catheter placed under local anaesthesia with 1% lidocaine injected subcutaneously. Animals were then anaesthetized with propofol (2–5 mg/kg IV), intubated and mechanically ventilated. General anaesthesia was maintained with inhalational isoflurane (1–2.5%) with fentanyl (5–20 μg/kg/min) infused as additional maintenance anaesthesia. A sterile limited left thoracotomy was made through the fourth intercoastal space, and epicardial echocardiography was performed to assess biventricular function and tricuspid and mitral valve competence. Tricuspid regurgitation grading included comprehensive evaluation of colour flow and continuous-wave Doppler and was categorized by an experienced echo sonographer as none or trace (0), mild (+1), moderate (+2) or moderately severe (+3) or severe (+4). The main pulmonary artery was then encircled with an umbilical tape before its bifurcation. While monitoring systemic and pulmonary pressures, the umbilical tape was tightened down with progressive clip approximations to the brink of haemodynamic stability as described previously [5]. Animals were kept monitored for 8 weeks with intermittent treatment with furosemide for evolving heart failure symptoms.

Terminal study

After completion of the recovery period, 17 surviving animals were brought back to the operating room and anaesthetized as outlined above. Ten health control sheep (CTL) also underwent the terminal procedure. The operative procedure was performed through a sternotomy, and epicardial echocardiography was repeated to assess biventricular function and valvular competence. While on cardiopulmonary bypass and with the heart beating, 6 (2 mm) sonomicrometry crystals (Sonometrics Corporation, London, Ontario, Canada) were implanted around the tricuspid annulus and 13 on the right ventricular epicardium with additional crystal at the right ventricular apex as shown in Fig. 1. A 1-mm crystal was placed on the central edge of the anterior tricuspid leaflet in 6 CTL and 8 PAB animals for the calculation of anterior leaflet tethering distance and angular excursion. Pressure transducers (PA4.5-X6; Konigsberg Instruments, Inc.) were placed in the right and left ventricle through the apex and in the right atrium. All animals were studied under open-chest experimental conditions 30 min after weaning from cardiopulmonary bypass.

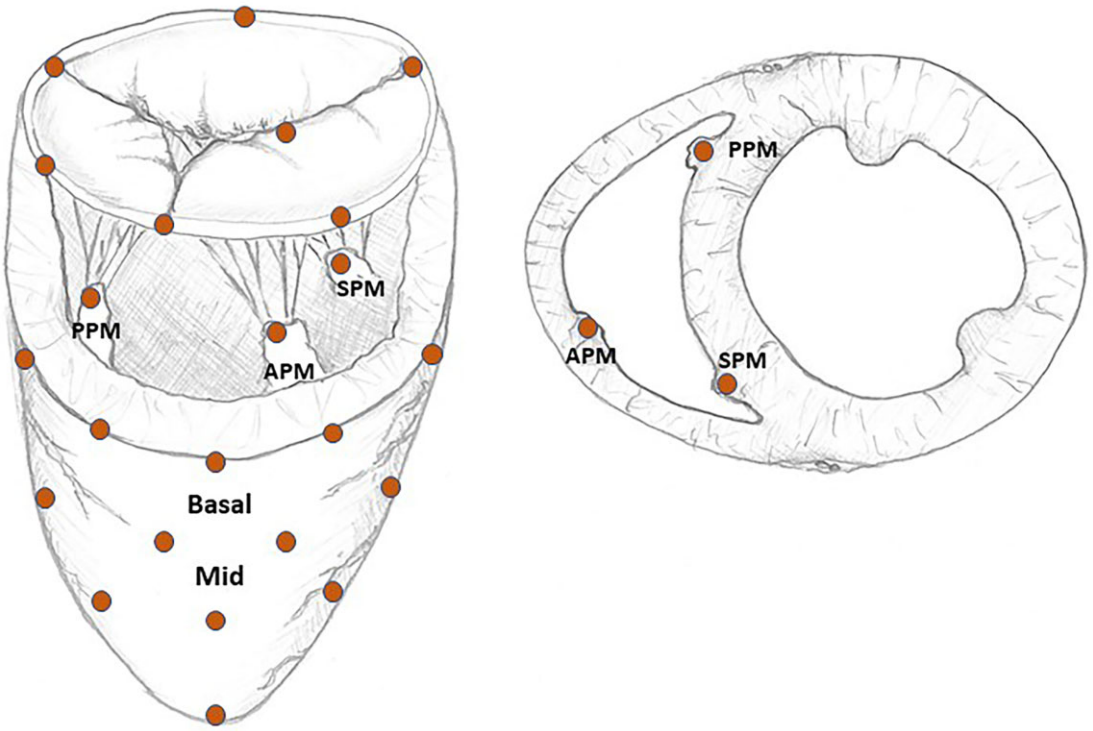

Figure 1: Schematic representation of the right ventricle with implanted sonomicrometry crystals around the tricuspid annulus and on the right ventricular epicardium, papillary muscle tips and central edge of the anterior leaflet. APM: anterior papillary muscle; PPM: posterior papillary muscle; SPM: septal papillary muscle.

At the conclusion of the experiment, the animals were euthanized by administering sodium pentothal (100 mg/kg IV). The heart was excised, and tricuspid valve leaflets from all animals were excised in continuity, photographed and divided for pentachrome histologic analysis and biomechanical testing. Leaflet area was calculated using custom imaging software and biomechanical testing was performed using biaxial device with tissue stiffness calculated as the tangent moduli to the tension–strain curves as described previously [6]. Excised tricuspid leaflets were formalin fixed for 24–72 h and processed on a Tissue-Tek VIP® 6 vacuum infiltration processor and paraffin embedded. Resulting tissue blocks were cut into 5-μM sections and stained with a modified Russell-Movat pentachrome stain. Representative micrographs were obtained by imaging on a Nikon Eclipse Ni microscope utilizing 4× and 10× objectives. Morphometric data were obtained in ImageJ (v1.53c). Measurements of cross-sectional thickness were obtained near the anatomical middle of the leaflet and fibrosa, spongiosa and atrialis regions were defined by a board-certified pathologist (Stephen Cohle). Quantification of mucin, collogen, elastin and nuclei were obtained in ImageJ utilizing macros developed to recognize their respective pentachrome stains.

Data acquisition

All sonomicrometry data were acquired using a Sonometrics Digital Ultrasonic Measurement System DS3 (Sonometrics Corporation) as previously described [7]. All sonomicrometry recordings were analysed with custom Matlab (Natick, MA) code. Parameter values were calculated at end systole (ES) and end diastole (ED). ED was defined as the time of the beginning of positive deflection in ECG voltage (R wave) while ES was determined as the time of maximum negative d*p*/d*t* of left ventricular pressure.

Data analysis

Right ventricular volume was determined using convex hull method based on epicardial, annular and papillary muscle tip crystals coordinates at ED (EDV) and ES and included myocardial volume. Right ventricle (RV) ejection fraction was calculated as (EDV − ESV)/EDV × 100%. Annular area and perimeter were determined from 3D coordinates of annular crystals. Anterior leaflet angle was defined as an angle made with annular plane by a vector leading from mid anterior annular crystal to anterior leaflet free edge crystal. Leaflet excursion angle was calculated as a difference between ED and ES angles. Tenting height was calculated as orthogonal distance from the annular plane to anterior leaflet free edge crystal at ES. Areal strain for the basal and mid-portion of the RV free wall was calculated based on epicardial crystals as recently described [7].

All the data are presented here as a mean with standard deviation. In addition, measured parameters were compared between CTL and PAB conditions using a two-tailed *t*-test for independent observations with a *P*-value of <0.05 considered significant. As this was our first study with the model of pulmonary banding, we felt that sufficient power was needed to detect a 20% increase in annular area that has been associated with FTR in prior studies with a standard deviation of 15%. With the assumption of ∼30% attrition rate and the power of 0.8, 19 animals in the experimental group were needed to arrive at 13 survivals and adequate sample size.

RESULTS

Three PAB animals died during the banding procedure one each from stroke, pulmonary artery haemorrhage and acute right

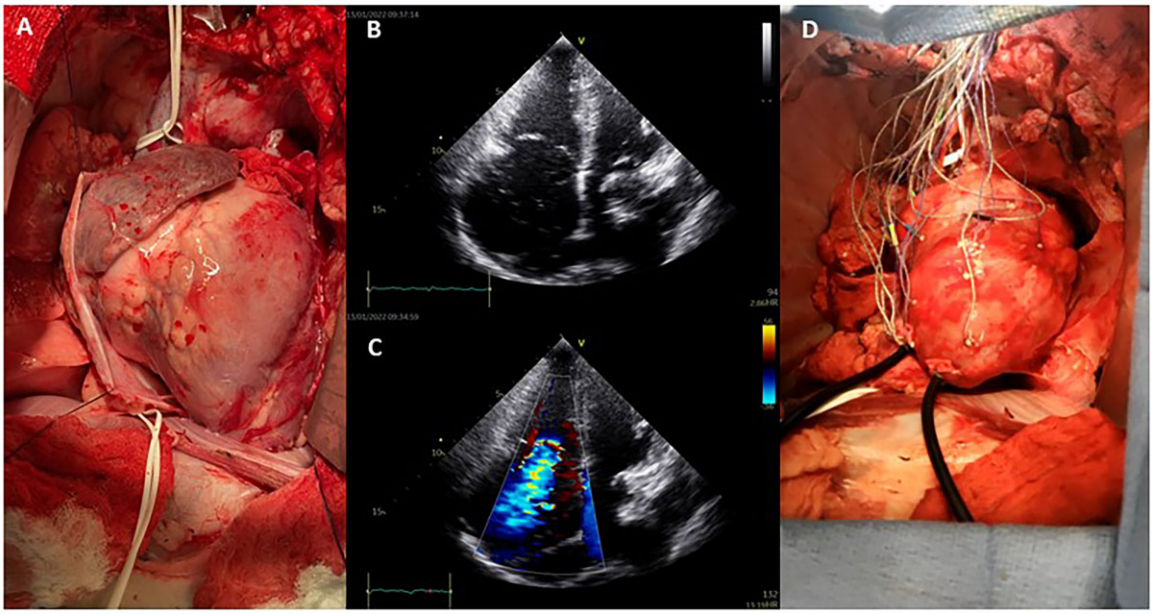

Figure 2: Intra-operative images of pulmonary artery banding animals. (**A**) Ovine heart after 8 weeks of pulmonary banding with remarkable right atrial and right ventricular enlargement. (**B**) Epicardial echocardiography demonstrating right ventricular and annular dilation as well as impressive right atrial dilation associated with pulmonary artery banding. (**C**) Colour Doppler confirming presence of severe functional tricuspid regurgitation. (**D**) Instrumented heart after weaning from cardiopulmonary bypass with implanted epicardial sonomicrometry crystals and right and left ventricular pressure transducers.

heart failure. The mean animal weight was 62 ± 5 and 63 ± 3 kg for CTL and PAB, respectively (P = 0.6). Systolic pulmonary artery pre-band pressure increased from 21 ± 2 to 62 ± 9 mmHg immediately after banding in PAB animals. The mean TR grade (+0–4) was 0.8 ± 0.4 and 3.2 ± 1.2 (P = 0.0001) for control and banded animals, respectively, while tricuspid annular diameter increased from 24.6 ± 2.3 to 31.2 ± 2.4 mm (P = 0.0001). Significant atrial and ventricular remodelling was observed in PAB animals as demonstrated in Fig. 2. Right ventricular fractional area change (57 ± 3 vs 38 ± 7%, P = 0.0001) and tricuspid annular plane systolic excursion (11.0 ± 0.9 vs 7.8 ± 1.3 mm, P = 0.00001) were significantly lower in PAB animals. Echocardiographically measured RV free wall thickness was 4.7 ± 0.5 mm in control and 5.4 ± 0.9 mm in banded animals (P = 0.04). Total weight of excised RV free wall myocardium was 50 ± 5 and 96 ± 21 g for CTL and PAB, respectively (P = 0.00001). In summary, PAB was associated with moderately severe TR, RV dysfunction and chamber remodelling and hypertrophy.

As demonstrated in Table 1, PAB animals had higher heart rates and right ventricular pressures while left ventricular and central venous pressures were did not differ from control. Right ventricular volume, annular area and area between the 3 papillary muscle tip crystals were substantially increased in PAB animals at ES increasing by 69%, 33% and 86% versus CTL, respectively. Inter-papillary distance increased between anterior–posterior and posterior–septal muscles and no apical displacement of papillary muscle tips away from the tricuspid annular plane was observed. These parameters of ventricular and subvalvular remodelling remained greater in banded animals throughout the cardiac cycle (Fig. 3) while RV free wall strain was significantly reduced at both basal and midventricular levels (Fig. 4). The above data reveal that functional TR was associated with remarkable myocardial dysfunction and RV and right atrium dilation as well as annular and subvalvular remodelling in our ovine model of PAB.

Anterior leaflet angular excursion during systole was significantly reduced in banded animals (7.4 ± 4.5° vs 23.8 ± 6.1°, P = 0.001; Fig. 5) while tenting height did not change at ES (12.3 ± 4.2 vs 9.0 ± 2.9 mm, P = 0.14). Surface area of all leaflets increased significantly with PAB with total leaflet area increasing from 806 ± 94 to 953 ± 148 mm^2 (P = 0.009) equating to an 18% enlargement (Table 2). Leaflet thickness increased in anterior and septal leaflets driven mainly by increased size of the fibrosa and the spongiosa layers. Leaflet tissue became stiffer in the circumferential direction in the septal and posterior leaflets with increasing radial stiffness in the anterior leaflet. Pentachrome staining (Fig. 6) revealed decreased leaflet cellularity associated with PAB as well as increased mucin content. Elastin and collagen content was not different from control.

DISCUSSION

Pathophysiology of FTR remains incompletely understood resulting in suboptimal clinical outcomes of isolated ring annuloplasty in patients with severe valve insufficiency [3, 4]. Results from the current ovine experiment demonstrate that annular enlargement is associated with severe functional TR, but subvalvular and leaflet remodelling are also remarkable and should not be ignored. These data behove multi-level interventions on the tricuspid valvular complex in the surgical treatment of severe functional FTR and may identify novel targets for surgical and potentially pharmacologic interventions.

The ovine model of pulmonary banding used in the study resulted in moderately severe FTR, which is consistent with prior studies [5]. Echocardiographic findings of our study demonstrated reduced RV function, chamber enlargement and annular dilatation all consistent with experimental observations of other investigators [8] and clinical reports in patients with functional TR [9]. In the setting of moderate or less insufficiency or isolated annular

Table 1: Haemodynamics and valvular complex geometry

	CTL (n = 10)	PAB (n = 17)	P-Value
HR (bpm)	88 ± 11	107 ± 15	0.007
LVP (mmHg)	98 ± 11	88 ± 17	0.20
RVP (mmHg)	30 ± 7	45 ± 14	0.015
CVP (mmHg)	12 ± 1	12 ± 2	0.55
RV EDV (ml)	126 ± 13	172 ± 34	0.0019
RV ESV (ml)	89 ± 7	149 ± 34	0.001
RV EF (%)	29 ± 6	13 ± 5	0.001
TAA (mm^2)	651 ± 109	865 ± 247	0.037
TAP (mm)	92 ± 8	110 ± 18	0.021
PMA (mm^2)	162 ± 51	302 ± 75	0.001
Inter-PM distance (mm)			
A–P	21.5 ± 4.1	28.8 ± 4.3	0.003
P–S	17.5 ± 4.1	22.8 ± 4.5	0.026
A–S	30.9 ± 5.1	31.6 ± 4.0	0.73
PM–TA plane distance (mm)			
A	22.6 ± 6.8	22.2 ± 4.8	0.89
P	18.2 ± 3.7	21.6 ± 4.5	0.095
S	19.4 ± 2.4	19.6 ± 3.4	0.88
RVA–TA plane (mm)	52.7 ± 6.8	55.8 ± 10.8	0.491

Values are represented as mean ± SD.

A: anterior; A–P: anterior–posterior; A–S: anterior–septal; CTL: control; CVP: central venous pressure; EDV: end diastolic volume; EF: ejection fraction; ESV: end-systolic volume; HR: heart rate; LVP: left ventricular pressure; P: posterior; PAB: pulmonary artery banding; PMA: papillary muscle area; P–S: posterior–septal; RV: right ventricle; RVA: right ventricular apex; RVP: right ventricular pressure; S: septal; SD: standard deviation; TA: tricuspid annulus; TAA: tricuspid annular area; TAP: tricuspid annular perimeter.

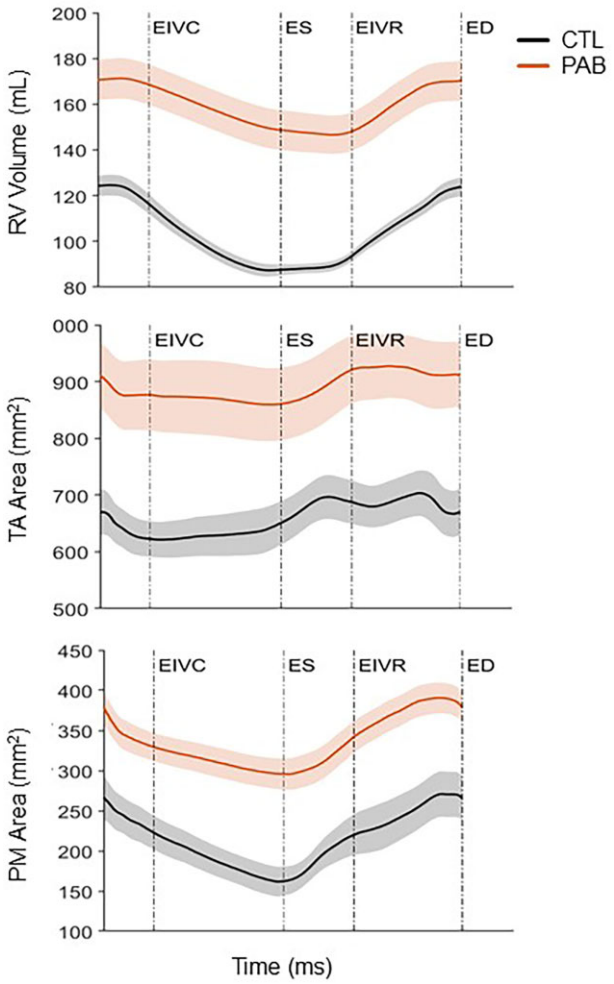

Figure 3: Group mean and standard deviation for right ventricular volume (top panel), tricuspid annular area (middle panel) and area between papillary muscle tips (bottom panel) throughout the cardiac cycle in control (CTL) and banded (pulmonary artery banding) animals. ED: end diastole; EIVC: end-isovolumic contraction; EIVR: end-isovolumic contraction; ES: end systole.

dilation of 40 mm regardless of TR, tricuspid annuloplasty provides durable and reproducible results [10]. However, it is postulated that when annular dilatation is observed with severe insufficiency, associated ventricular and subvalvular geometric changes have become very advanced so as to deem isolated annular reduction ineffective [11]. In our banded animals, right ventricular volume increase was almost twice as great as annular area dilation relative to control animals corroborating this notion. This form of ventricular remodelling is consistent with elliptical RV chamber dilation that has been described echocardiographically in patients with pulmonary hypertension. However, lack of apical papillary muscle displacement or evidence of leaflet tethering suggest that features of conical remodelling seem with atriogenic FTR. The hybrid remodelling demonstrated in our experiment may be due to limited follow-up and differences between clinical pulmonary hypertension which evolves over years versus acute increase with pulmonary banding in our model. Right ventricular dilation has been shown to be associated with altered subvalvular geometry and leaflet tethering in patients with severe FTR [12], and our observation of increased papillary muscle area in PAB animals support these findings. Annular reduction alone is unlikely to correct these geometric perturbations, and data from isolated pig hearts induced with severe FTR have shown that tricuspid annuloplasty reduces but does not eliminate TR suggesting that subvalvular interventions may be needed [13]. *In vitro* studies have demonstrated that isolated papillary muscle displacement can also cause TR [14], and we observed impressive displacement of papillary muscle tip position associated with PAB as illustrated by almost a doubling of papillary muscle area. These findings support experimental *ex vivo* [15] and early clinical [16] attempts at correction of subvalvular perturbations through papillary muscle approximation. Matsumiya *et al.* [17] approximated anterior and posterior papillary muscle to supplement ring annuloplasty in 7 high-risk patients with severe TR and found reduced leaflet tethering and good short-term results. The directionality of papillary approximation in this small clinical study is consistent with our data as we observed the largest inter-papillary muscle distance increase between anterior and posterior papillary muscle tips.

Clinically, the sum of annular, ventricular and subvalvular geometric alterations ultimately leads to leaflet tethering and valvular insufficiency. Anterior leaflet motion in banded sheep revealed significantly restricted systolic angular excursion although end-systolic tethering did not change. However, until recently [18], leaflet tissue has been considered inert and not an active participant in the pathophysiology of FTR. In our study, leaflet area increased significantly with pulmonary banding suggesting active tissue remodelling. Our previous studies in sheep with FTR induced by rapid pacing revealed 30% area increase of the anterior leaflet [6] which is in line with approximately a 20% increase observed in the current study. Although the geometric alterations in the annulus and subvalvular structures observed herein have been reported in other experimental and clinical studies, the

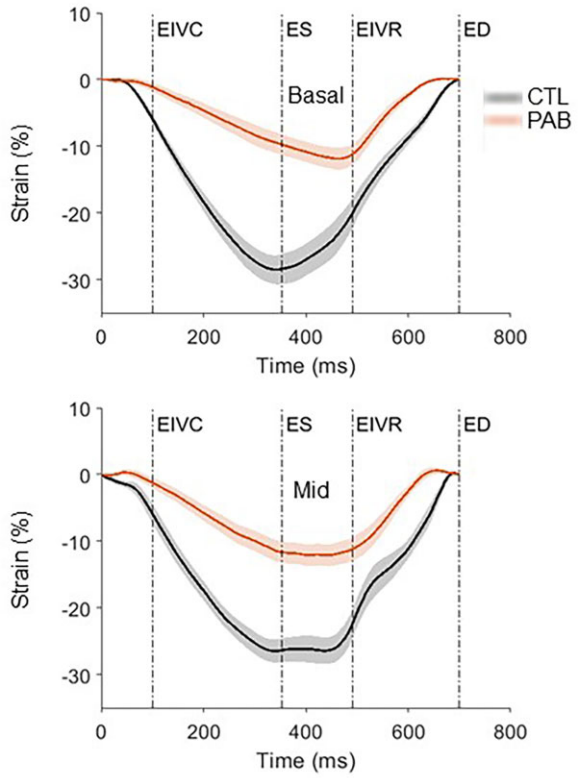

Figure 4: Group mean and standard deviation for right ventricular free wall areal strain at basal (top panel) and mid-ventricle (bottom panel) throughout the cardiac cycle in control (CTL) and banded (pulmonary artery banding) animals. ED: end diastole; EIVC: end-isovolumic contraction; EIVR: end-isovolumic contraction; ES: end systole.

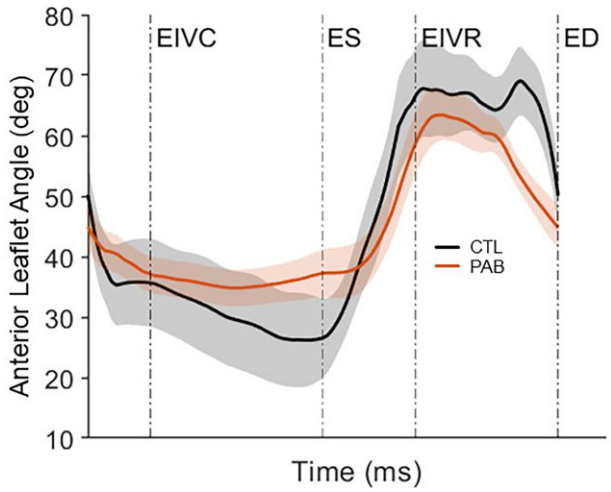

Figure 5: Group mean and standard deviation of anterior leaflet angle throughout the cardiac cycle in control (CTL) and banded (pulmonary artery banding) animals. ED: end diastole; EIVC: end-isovolumic contraction; EIVR: end-isovolumic contraction; ES: end systole.

alterations in leaflet size and histology are novel and corroborate echocardiographic findings in patients. Afilalo *et al.* [18] found that in patients with pulmonary hypertension, TR severity was predicted by inadequate increase in tricuspid leaflet area demonstrating clinical significance of tricuspid leaflet remodelling and corroborating the current data. Furthermore, attenuated leaflet

Table 2: Leaflet characteristics

	Control	PAB	*P*-Value
Leaflet area (mm^2)			
Anterior	303 ± 56	363 ± 79	0.046
Posterior	254 ± 47	303 ± 49	0.018
Septal	248 ± 36	287 ± 51	0.041
Leaflet thickness (μM)			
Anterior	559 ± 156	736 ± 213	0.052
Posterior	453 ± 128	613 ± 304	0.15
Septal	538 ± 142	868 ± 276	0.002
Atrialis (μM)			
Anterior	73 ± 17	71 ± 33	0.83
Posterior	69 ± 31	63 ± 26	0.59
Septal	61 ± 25	86 ± 41	0.16
Fibrosa (μM)			
Anterior	160 ± 59	218 ± 71	0.061
Posterior	137 ± 40	207 ± 82	0.029
Septal	163 ± 43	209 ± 43	0.011
Spongiosa (μM)			
Anterior	325 ± 104	447 ± 172	0.084
Posterior	246 ± 95	344 ± 246	0.27
Septal	314 ± 115	589 ± 254	0.005
Radial stiffness (N/m)			
Anterior	613 ± 270	789 ± 156	0.081
Posterior	598 ± 139	604 ± 152	0.928
Septal	635 ± 293	627 ± 252	0.945
Circumferential stiffness (N/m)			
Anterior	1039 ± 263	1192 ± 339	0.295
Posterior	640 ± 110	937 ± 339	0.031
Septal	535 ± 164	797 ± 228	0.013

Values are represented as mean ± SD.
PAB: pulmonary artery banding; SD: standard deviation.

enlargement was found to contribute to functional mitral regurgitation in sheep [19], while surgical anterior leaflet augmentation has demonstrated good efficacy in selected patients with leaflet tethering and severe FTR [20]. Conversely, short leaflet length was found to be a predictor of residual valve insufficiency after surgical repair of functional TR with ring annuloplasty [21]. However, the physiologic stimuli of adaptive leaflet growth and compensation remain to be defined.

In addition to increased leaflet area, we found that leaflets in PAB animals became thicker and stiffer consistent with findings in ovine FTR associated with rapid ventricular pacing [6]. Utsunomiya *et al.* [21] also found TV leaflet thickness to be a predictor of residual TR after surgical repair, and mitral leaflets were reported to be 1.4-fold thicker in sheep with dilated cardiomyopathy and mitral regurgitation versus cardiomyopathy alone [22]. Normal ovine tricuspid leaflets have been found to have variable microstructure and mechanical properties [23] with layer specific biomechanics reported in porcine anterior tricuspid leaflets [24]. Tricuspid leaflet response to pulmonary banding was likewise heterogenous as evidenced by our biomechanical findings although fibrosa and spongiosa layers of all leaflets were the consistent drivers of leaflet thickening. These alterations may be mediated by tethering forces as thickening of the spongiosa layer of mitral leaflets from experimentally induced *in vivo* stretch of the valve without associated insufficiency was observed by Dal-Bianco *et al.* [25]. It follows that increased mucin content found in our banded animals may be directly related to spongiosa hypertrophy and leaflet tethering. However, increased ventricular pressure may also contribute as *ex vivo* study of porcine tricuspid

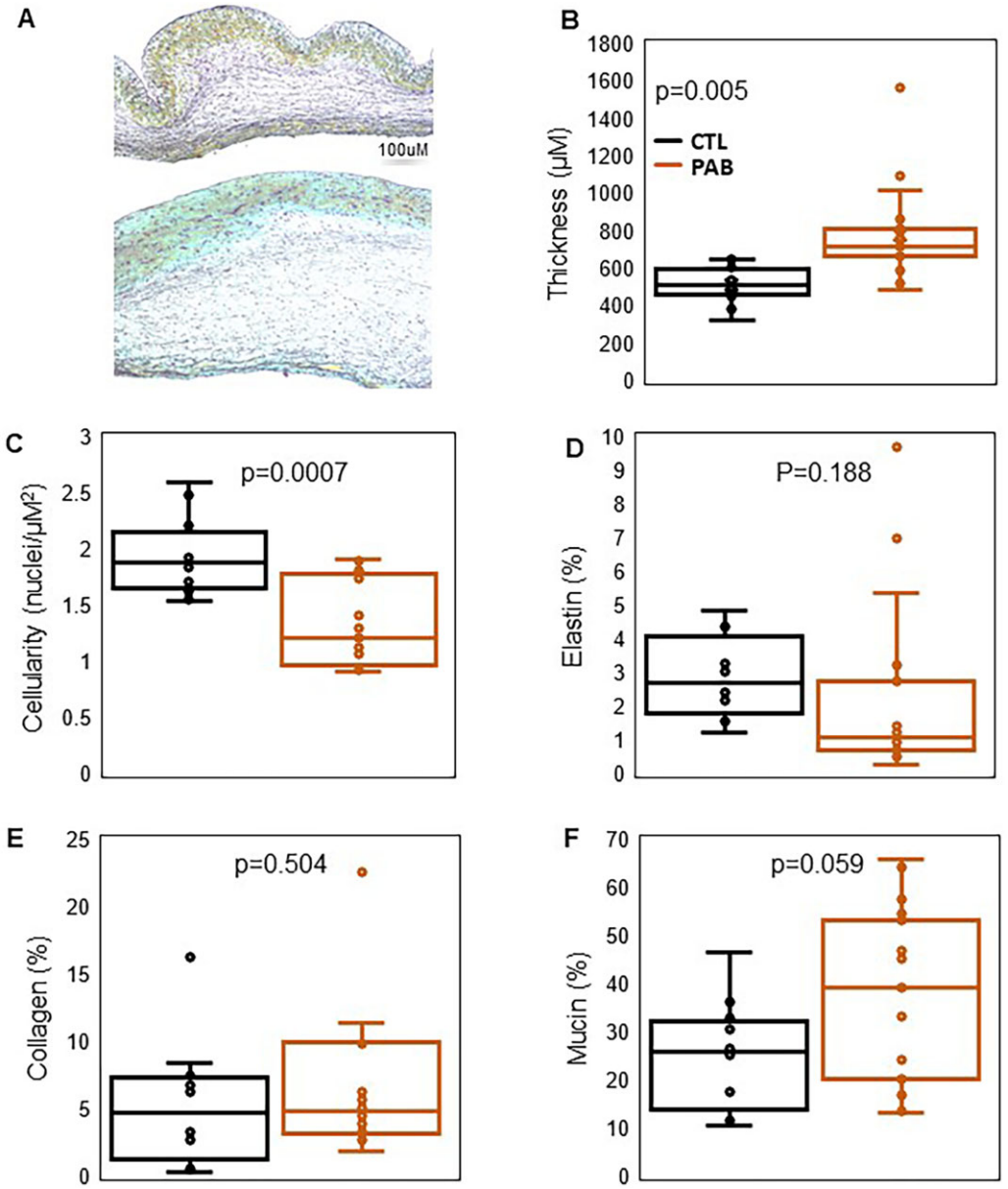

Figure 6: Pentachrome staining at 10× magnification of anterior tricuspid valve leaflet from control (top) and pulmonary artery banded (bottom) animal (**A**). Group mean and standard deviation for control (CTL) and pulmonary artery banding (pulmonary artery banding) animals of leaflet thickness (**B**), cellularity (**C**), elastin content (**D**), collagen content (**E**) and mucin content (**F**).

valves revealed pressure induced changes in the extracellular matrix [26]. Furthermore, the histologic and ultrastructural alterations observed in the leaflet tissue may be a result of TR induced turbulence and tissue injury with subsequent repair response. Defining the molecular pathways responsible for leaflet remodelling may offer novel adjunctive therapeutic targets for treatment of FTR, and innovative studies of post-infarction ovine mitral valves have shown this to be a possibility as Losartan treatment was found to modulate fibrotic changes in the valve while maintaining adaptive growth through inhibition of TGF-B [27]. Such data are at this time lacking for the tricuspid valve.

The integrated pathophysiology model of FTR described in our experiment warrants comparison to prior studies investigating pathophysiology function mitral regurgitation. We found annular and subvalvular geometric alterations similar to those described in ovine chronic functional MR [28] and in the clinical literature. Similarly, we have previously described leaflet remodelling associated with FMR in dilated cardiomyopathy [29] further corroborating current findings on the right side of the heart. Although leaflet tethering has been shown clinically to be associated with both FMR and FTR, it is often extrapolated to apical displacement of papillary muscle tips which we have not observed either in ovine FTR or FMR although lateral displacement was present. Clinically, FTR is most frequently a result of left-sided valvular dysfunction and pulmonary hypertension whereas FMR is associated with myocardial dysfunction either from coronary artery disease or cardiomyopathy. Central to both, is the notion of lack of structural damage to the valve apparatus; yet, our current and past studies suggest that the 'normal' appearing leaflets of functional atrioventricular valve insufficiency may indeed not be so.

Limitations

The results of our study must be viewed from a perspective of several important limitations. The chosen model of right ventricular failure and FTR was afterload induced with a pulmonary band and as such does not reflect clinical reality. However, experimental afterload-based models may be more reliable to induce FTR as clinical studies have shown that volume overload even when associated with RV dilation does not lead to significant valvular insufficiency [30]. Furthermore, clinical FTR is predominantly associated with left-sided valve lesions which were not duplicated in our model. As such, our model of FTR reflects that which is clinically associated with pulmonary diseases or chronic pulmonary thromboembolism rather than the FTR that is seen in surgical practice. To this end, clinical extrapolation of these experimental results to clinical practice should be made with great caution. FTR usually develops over years in patients and the 8-week duration of our experiment represents and accelerated course. However, the morphological changes in the tricuspid valve apparatus found in our model reflect clinical findings.

CONCLUSION

In conclusion, our model of FTR induced by 8 weeks of PAB was associated with echocardiographic findings reported in patients with severe FTR. Our detailed analysis of the tricuspid valve complex revealed significant annular, ventricular and subvalvular and leaflet remodelling to be associated with severe FTR. These data add impetus to a more comprehensive approach to surgical repair of FTR beyond reductive ring annuloplasty while further investigations into the molecular mechanisms of leaflet remodelling may offer pharmacologic targets for early treatment of FTR.

ACKNOWLEDGEMENT

Dr Artur Iwasieczko was supported by the Peter C and Pat Cook Endowed Clinical Research Fellowship.

Funding

The study was funded by internal grant from the Meijer Heart and Vascular Institute at Spectrum Health and National Institute of Health NHLBI 1R01HL165251-01 (Tomasz A. Timek and Manuel Rausch).

Conflict of interest: none declared.

DATA AVAILABILITY

Data are available on request. The data underlying this article will be shared on reasonable request to the corresponding author.

Author contributions

Artur Iwasieczko: Conceptualization; Formal analysis; Investigation. **Manikantam Gaddam:** Formal analysis; Software. **Boguslaw Gaweda:** Conceptualization; Formal analysis; Investigation; Methodology. **Austin Goodyke:** Data curation; Formal analysis. **Mrudang Mathur:** Data curation. **Chien-Yu Lin:** Data curation. **Joseph Zagorski:** Investigation; Methodology. **Monica Solarewicz:** Project administration; Resources. **Stephen Cohle:** Methodology; Resources. **Manuel Rausch:** Conceptualization; Formal analysis. **Tomasz A. Timek:** Conceptualization; Formal analysis; Funding acquisition.

Reviewer information

European Journal of Cardio-Thoracic Surgery thanks Francesco Nappi and the other anonymous reviewer(s) for their contribution to the peer review process of this article.

REFERENCES

[1] Enriquez-Sarano M, Messika-Zeitoun D, Topilsky Y, Tribouilloy C, Benfari G, Michelena H. Tricuspid regurgitation is a public health crisis. Prog Cardiovasc Dis 2019;62:447–51.
[2] Otto CM, Nishimura RA, Bonow RO, Carabello BA, Erwin JP 3rd, Gentile F *et al.*; ACC/AHA Joint Committee Members. 2020 ACC/AHA guideline for the management of patients with valvular heart disease: a report of the American College of Cardiology/American Heart Association Joint Committee on Clinical Practice Guidelines. J Thorac Cardiovasc Surg 2021;162:e183–e353.
[3] Calafiore AM, Foschi M, Kheirallah H, Alsaied MM, Alfonso JJ, Tancredi F *et al.* Early failure of tricuspid annuloplasty. Should we repair the tricuspid valve at an earlier stage? The role of right ventricle and tricuspid apparatus. J Card Surg 2019;34:404–11.
[4] Navia JL, Nowicki ER, Blackstone EH, Brozzi NA, Nento DE, Atik FA *et al.* Surgical management of secondary tricuspid valve regurgitation: annulus, commissure, or leaflet procedure? J Thorac Cardiovasc Surg 2010; 139:1473–82.e5.
[5] Verbelen T, Burkhoff D, Kasama K, Delcroix M, Rega F, Meyns B. Systolic and diastolic unloading by mechanical support of the acute vs the chronic pressure overloaded right ventricle. J Heart Lung Transplant 2017;36:457–65.
[6] Meador WD, Mathur M, Sugerman GP, Malinowski M, Jazwiec T, Wang X *et al.* The tricuspid valve also maladapts as shown in sheep with biventricular heart failure. eLife 2020;9:e63855.
[7] Jazwiec T, Malinowski M, Ferguson H, Wodarek J, Quay N, Bush J *et al.* Effect of variable annular reduction on functional tricuspid regurgitation and right ventricular dynamics in an ovine model of tachycardia-induced cardiomyopathy. J Thorac Cardiovasc Surg 2021;161: e277–e286.
[8] Nguyen-Truong M, Liu W, Boon J, Nelson B, Easley J, Monnet E *et al.* Establishment of adult right ventricle failure in ovine using a graded, animal-specific pulmonary artery constriction model. Animal Model Exp Med 2020;3:182–92.
[9] Prihadi EA, Delgado V, Leon MB, Enriquez-Sarano M, Topilsky Y, Bax JJ. Morphologic types of tricuspid regurgitation: characteristics and prognostic implications. JACC Cardiovasc Imaging 2019;12:491–9.
[10] Gammie JS, Chu MWA, Falk V, Overbey JR, Moskowitz AJ, Gillinov M et al; CTSN Investigators. Concomitant tricuspid repair in patients with degenerative mitral regurgitation. N Engl J Med 2022;386:327–39.
[11] Dreyfus GD, Martin RP, Chan KM, Dulguerov F, Alexandrescu C. Functional tricuspid regurgitation: a need to revise our understanding. J Am Coll Cardiol 2015;65:2331–6.
[12] van Rosendael PJ, Joyce E, Katsanos S, Debonnaire P, Kamperidis V, van der Kley F *et al.* Tricuspid valve remodelling in functional tricuspid regurgitation: multidetector row computed tomography insights. Eur Heart J Cardiovasc Imaging 2016;17:96–105.
[13] Spinner EM, Shannon P, Buice D, Jimenez JH, Veledar E, Del Nido PJ et al *in vitro* characterization of the mechanisms responsible for functional tricuspid regurgitation. Circulation 2011;124:920–9.
[14] Spinner EM, Lerakis S, Higginson J, Pernetz M, Howell S, Veledar E *et al.* Correlates of tricuspid regurgitation as determined by 3D echocardiography: pulmonary arterial pressure, ventricle geometry, annular dilatation, and papillary muscle displacement. Circ Cardiovasc Imaging 2012; 5:43–50.
[15] Yamauchi H, Vasilyev NV, Marx GR, Loyola H, Padala M, Yoganathan AP *et al.* Right ventricular papillary muscle approximation as a novel technique of valve repair for functional tricuspid regurgitation in an *ex vivo* porcine model. J Thorac Cardiovasc Surg 2012;144:235–42.

[16] Al-Attar N, Hvass U. Right papillary muscle sling: proof of concept and pilot clinical experience. Eur J Cardiothorac Surg 2013;43:e187-9–e189.
[17] Matsumiya G, Kohno H, Matsuura K, Sakata T, Tamura Y, Watanabe M et al Right ventricular papillary muscle approximation for functional tricuspid regurgitation associated with severe leaflet tethering. Interact CardioVasc Thorac Surg 2018;26:700–2.
[18] Afilalo J, Grapsa J, Nihoyannopoulos P, Beaudoin J, Gibbs JS, Channick RN *et al.* Leaflet area as a determinant of tricuspid regurgitation severity in patients with pulmonary hypertension. Circ Cardiovasc Imaging 2015; 8. doi:10.1161/CIRCIMAGING.114.002714.
[19] Marsit O, Clavel MA, Côté-Laroche C, Hadjadj S, Bouchard MA, Handschumacher MD *et al.* Attenuated mitral leaflet enlargement contributes to functional mitral regurgitation after myocardial infarction. J Am Coll Cardiol 2020;75:395–405.
[20] Dreyfus GD, Raja SG, John Chan KM. Tricuspid leaflet augmentation to address severe tethering in functional tricuspid regurgitation. Eur J Cardiothorac Surg 2008;34:908–10.
[21] Utsunomiya H, Itabashi Y, Mihara H, Kobayashi S, De Robertis MA, Trento A *et al.* Usefulness of 3D echocardiographic parameters of tricuspid valve morphology to predict residual tricuspid regurgitation after tricuspid annuloplasty. Eur Heart J Cardiovasc Imaging 2017;18:809–17.
[22] Beaudoin J, Handschumacher MD, Zeng X, Hung J, Morris EL, Levine RA *et al.* Mitral valve enlargement in chronic aortic regurgitation as a compensatory mechanism to prevent functional mitral regurgitation in the dilated left ventricle. J Am Coll Cardiol 2013;61:1809–16.
[23] Meador WD, Mathur M, Sugerman GP, Jazwiec T, Malinowski M, Bersi MR *et al.* A detailed mechanical and microstructural analysis of ovine tricuspid valve leaflets. Acta Biomater 2020;102:100–13.
[24] Kramer KE, Ross CJ, Laurence DW, Babu AR, Wu Y, Towner RA *et al.* An investigation of layer-specific tissue biomechanics of porcine atrioventricular valve anterior leaflets. Acta Biomater 2019;96:368–84.
[25] Dal-Bianco JP, Aikawa E, Bischoff J, Guerrero JL, Handschumacher MD, Sullivan S *et al.* Active adaptation of the tethered mitral valve: insights into a compensatory mechanism for functional mitral regurgitation. Circulation 2009;120:334–42.
[26] Pant AD, Thomas VS, Black AL, Verba T, Lesicko JG, Amini R *et al.* Pressure-induced microstructural changes in porcine tricuspid valve leaflets. Acta Biomater 2018;67:248–58.
[27] Bartko PE, Dal-Bianco JP, Guerrero JL, Beaudoin J, Szymanski C, Kim DH *et al.*; Leducq Transatlantic Mitral Network. Effect of losartan on mitral valve changes. J Am Coll Cardiol 2017;70:1232–44.
[28] Tibayan FA, Rodriguez F, Zasio MK, Bailey L, Liang D, Daughters GT *et al.* Geometric distortions of the mitral valvular-ventricular complex in chronic ischemic mitral regurgitation. Circulation 2003;108:II116–21.
[29] Timek TA, Lai DT, Dagum P, Liang D, Daughters GT, Ingels NB, Jr, *et al.* Mitral leaflet remodeling in dilated cardiomyopathy. Circulation 2006; 114: I518–23.
[30] Offen SM, Baker D, Puranik R, Celermajer DS. Right ventricular volume and its relationship to functional tricuspid regurgitation. Int J Cardiol Heart Vasc 2022;38:100940.